Neuro-Swarm computational heuristic for solving a nonlinear second order coupled Emden-Fowler model

Zulqurnain Sabir[1,a], Muhammad Asif Zahoor Raja[2,b], Dumitru Baleanu[3,4,c], Juan L.G. Guirao[5,d]

[1]Department of Mathematics and Statistics, Hazara University, Mansehra, Pakistan
[a]Email: zulqurnain_maths@hu.edu.pk
[2]Future Technology Research Center, National Yunlin University of Science and Technology, 123 University Road, Section 3, Douliou, Yunlin 64002, Taiwan, R.O.C.
[b]Email: rajamaz@yuntech.edu.tw
[3]Department of Mathematics, Cankaya University, Ankara, Turkey d Institute of Space Sciences, Magurele, Romania
[c]Email: dumitru@cankaya.edu.tr
[4]Institute of Space Sciences, Magurele, Romania

[5]Department of Applied Mathematics and Statistics, Technical University of Cartagena, Hospital de Marina 30203-Cartagena, Spain

[d]Email: juan.garcia@upct.es

Abstract: The aim of the current study is to present the numerical solutions of a nonlinear second order coupled Emden-Fowler equation by developing a neuro-swarming based computing intelligent solver. The feedforward artificial neural networks (ANNs) are used for modelling and optimization is carried out by the local/global search competences of particle swarm optimization (PSO) aided with capability of interior-point method (IPM), i.e., ANNs-PSO-IPM. In ANNs-PSO-IPM, a mean square error based objective function is designed for nonlinear second order coupled Emden-Fowler (EF) equations and then optimized using the combination of PSO-IPM. The inspiration to present the ANNs-PSO-IPM comes with a motive to depict a viable, detailed and consistent framework to tackle with such stiff/nonlinear second order coupled EF system. The ANNs-PSO-IP scheme is verified for different examples of the second order nonlinear-coupled EF equations. The achieved numerical outcomes for single as well as multiple trials of ANNs-PSO-IPM are incorporated to validate the reliability, viability and accuracy.

Keywords: Coupled Emden-Fowler model; Interior-point algorithm; Neural networks; Numerical computing.

Abbreviations	
EF	Emden-Fowler

ANNs	Artificial neural networks
PSO	particle swarm optimization
IPM	interior-point method
RMSE	Root Mean Square Error
VAF	Variance Account For
SI	Semi Interquartile
EVAF	Error in VAF
PSO-IPM	PSO aided with IPM
ANNs-PSO-IPM	ANNs optimized with PSO and IPM
MIN	Minimum
SD	Standard deviation

1. Introduction

The historical Emden-Fowler (EF) system is considered very important for the research community because of singularity at the origin and has various applications in wide-ranging fields of applied science and engineering. Some well-known applications are catalytic diffusion reactions using the error estimate models [1], stellar configuration [2], density profile of gaseous star [3], spherical annulus [4], isotropic continuous media [5], extrinsic thermionic maps [6], the theory of electromagnetic [7] and morphogenesis [8]. Due to the specialty of the singular point and extensive applications, the researcher has always shown keen interest to solve these models all the time. These models are not easy to solve due of this singular model, nonlinearity and stiff nature and only a few techniques are available in the literature to solve these models. Few of them are Legendre spectral wavelets scheme [9], Adomian decomposition scheme [10], Haar quasilinearization wavelet scheme [11-12], an analytic algorithm approach [13], rational Legendre approximation scheme [14], modified variational iteration scheme [15], differential transformation scheme [16], fourth-order B-spline collocation scheme [17], Chebyshev operational matrix scheme [18] and variation of parameters scheme with an auxiliary parameter [19]. Beside these the numerical methodologies introduced in [20-25] can be exploited for EF equations-based systems.

All these mentioned schemes have their specific merits/advantages and demerits/imperfections, whereas, soft computing stochastic solver is used to manipulate the artificial neural networks (ANNs) strength optimized by global/local search proficiencies of particle swarm optimization (PSO) and interior-point method (IPM), i.e., ANNs-PSO-IPM, have not been implemented for the nonlinear coupled EF model of second kind. The researchers have been generally practiced the numerical computing meta-heuristic schemes along with the neural network strengths for solving the various mathematical linear/nonlinear models [26-32]. Few recent applications of the stochastic solvers are financial market forecasting [33], food chain model [34], nonlinear smoking models [35], nonlinear fractional Lane–Emden systems [36], nonlinear second-order Lane–Emden pantograph delay differential systems [37], peristaltic motion of a third-grade fluid involving planar channel [38], nonlinear predator-prey system [39], elliptic partial differential model [40], mathematical form of the Leptospirosis system [41], HIV mathematical models [42-43], nonlinear multiple singularities based systems [44], singular Thomas-Fermi equation [45], heartbeat dynamics [46], a corneal model for eye surgery [47-48] and heat conduction model of the human head [49]. These proposed stochastic solvers verified the values of the exactness, convergence, and accurateness of the ANNs-PSO-IPM.

Keeping in view all the consequences of above proposals, authors are interested to exploit the numerical stochastic solvers for consistent, stable, and efficient scheme for nonlinear second order coupled EF system. The literature form of the coupled EF model of second kind is written as [50]:

$$\begin{cases} \dfrac{d^2U}{d\Psi^2}+\dfrac{\alpha}{\Psi}\dfrac{dU}{d\Psi}+H_1(\Psi)G_1(U,V)=F_1(\Psi),\ \ U(0)=A,\ \dfrac{dU(0)}{d\Psi}=0, \\ \dfrac{d^2V}{d\Psi^2}+\dfrac{\beta}{\Psi}\dfrac{dV}{d\Psi}+H_2(\Psi)G_2(U,V)=F_2(\Psi),\ V(0)=B,\ \dfrac{dV(0)}{d\Psi}=0, \end{cases} \tag{1}$$

Where G_1 and G_2 are the nonlinear functions, α and β are the constants, while F_1 and F_2 are designated as a source functions. The aim of this current study is to solve the model given in equation (1) through intelligent computing schemes based on ANN-PSO-IP scheme. Some inventive inspiration of the current study is presented as:

- A neuro-swarm novel intelligent computing ANNs-PSO-IPM is designed and presented to solve second order nonlinear coupled EF model.
- The overlapping results of the proposed ANNs-PSO-IPM with the exact solutions for four different examples of the nonlinear-coupled EF based model of second kind establish the consistency, exactness and convergence.
- Ratification of the precise performance is authenticated via statistical calculations/observations on multiple runs of ANN-PSO-IP scheme in terms of root mean square error, Variance Account For, Semi Interquartile Range and Theil's inequality coefficient metrics.
- Beside essentially precise continuous results on whole interval, ease in the concept, stability, the smooth implementable practice and extendibility are well-intentioned declarations for the presented ANNs-PSO-IPM.

The remaining forms of the present work are shown as; Sec 2 presents the detailed methodology of the neural networks using the optimization process ANNs-PSO-IP scheme. Sec 3 presents the performance measures. Sec 4 indicates the numerical measures of the ANNs-PSO-IPM together with the statistical measures. Finally, some concluding remarks along with future work plans are described.

2. Methodology

This section presents the design of ANNs-PSO-IPM for second order nonlinear coupled EF model in two stages as given below:

Stage 1: A mean square error based objective/fitness function is constructed for nonlinear coupled EF model

Stage 2: The training/learning of the networks is presented with the help of hybrid PSO-IPM.

2.1 ANNs modeling

The neural networks are extensively applied to solve the diverse applications arising in sundry domains of engineering and applied sciences [51-54]. The proposed results are indicated as $\hat{U}(\Psi)$

and $\hat{V}(\Psi)$, while $\frac{d^n\hat{U}}{d\Psi^n}$ and $\frac{d^n\hat{V}}{d\Psi^n}$ are the derivatives of n[th] order, respectively and are given as follows:

$$\left[\hat{U}(\Psi),\hat{V}(\Psi)\right]=\left[\sum_{i=1}^{m}\phi_{U,i}P(w_{U,i}\Psi+a_{U,i}),\ \sum_{i=1}^{m}\phi_{V,i}P(w_{V,i}\Psi+a_{V,i})\right],$$
$$\left[\frac{d^n\hat{U}}{d\Psi^n},\frac{d^n\hat{V}}{d\Psi^n}\right]=\left[\sum_{i=1}^{m}\phi_{U,i}\frac{d^n}{d\Psi^n}P(w_{U,i}\Psi+a_{U,i}),\ \sum_{i=1}^{m}\phi_{V,i}\frac{d^n}{d\Psi^n}P(w_{V,i}\Psi+a_{V,i})\right], \quad (2)$$

where ϕ, w and a are the unknown weight vectors, while m and n are the number of neurons and the order of derivative, respectively.

$\boldsymbol{W}=[\boldsymbol{W}_U,\boldsymbol{W}_V]$, for $\boldsymbol{W}_U=[\boldsymbol{\phi}_U,\boldsymbol{w}_U,\boldsymbol{\alpha}_U]$ and $\boldsymbol{W}_V=[\boldsymbol{\phi}_V,\boldsymbol{w}_V,\boldsymbol{\alpha}_V]$. The weight vector components are shown as:

$$\boldsymbol{\phi}_U=[\phi_{U,1},\phi_{U,2},...,\phi_{U,m}],\quad \boldsymbol{w}_U=[w_{U,1},w_{U,2},...,w_{U,m}],\quad \boldsymbol{a}_U=[a_{U,1},a_{U,2},...,a_{U,m}],$$
$$\boldsymbol{\phi}_V=[\phi_{V,1},\phi_{V,2},...,\phi_{V,m}],\quad \boldsymbol{w}_V=[w_{V,1},w_{V,2},...,w_{V,m}],\quad \boldsymbol{a}_V=[a_{V,1},a_{V,2},...,a_{V,m}].$$

The log-sigmoid $P(\Psi)=\frac{1}{\left(1+\mathrm{e}^{-\Psi}\right)}$ is as an activation function and the simplified form of the network (2) using the $\hat{U}(\Psi)$ and $\hat{V}(\Psi)$ along with their derivatives are shown as:

$$\left[\hat{U}(\Psi),\hat{V}(\Psi)\right]=\left[\sum_{i=1}^{m}\frac{\phi_{U,i}}{1+e^{-\left(w_{U,i}\Psi+a_{U,i}\right)}},\ \sum_{i=1}^{m}\frac{\phi_{V,i}}{1+e^{-\left(w_{V,i}\Psi+a_{V,i}\right)}}\right],$$
$$\left[\frac{d\hat{U}}{d\Psi},\frac{d\hat{V}}{d\Psi}\right]=\left[\sum_{i=1}^{m}\frac{\phi_{U,i}w_{U,i}e^{-\left(w_{U,i}\Psi+a_{U,i}\right)}}{\left(1+e^{-\left(w_{U,i}\Psi+a_{U,i}\right)}\right)^2},\ \sum_{i=1}^{m}\frac{\phi_{V,i}w_{V,i}e^{-\left(w_{V,i}\Psi+a_{V,i}\right)}}{\left(1+e^{-\left(w_{V,i}\Psi+a_{V,i}\right)}\right)^2}\right],$$
$$\left[\frac{d^2\hat{U}}{d\Psi^2},\frac{d^2\hat{V}}{d\Psi^2}\right]=\left[\begin{array}{l}\sum_{i=1}^{m}\phi_{U,i}w_{U,i}^2\left\{\frac{2e^{-2\left(w_{U,i}\Psi+a_{U,i}\right)}}{\left(1+e^{-\left(w_{U,i}\Psi+a_{U,i}\right)}\right)^3}-\frac{e^{-\left(w_{U,i}\Psi+a_{U,i}\right)}}{\left(1+e^{-\left(w_{U,i}\Psi+a_{U,i}\right)}\right)^2}\right\},\\ \sum_{i=1}^{m}\phi_{V,i}w_{V,i}^2\left\{\frac{2e^{-2\left(w_{V,i}\Psi+a_{V,i}\right)}}{\left(1+e^{-\left(w_{V,i}\Psi+a_{V,i}\right)}\right)^3}-\frac{e^{-\left(w_{V,i}\Psi+a_{V,i}\right)}}{\left(1+e^{-\left(w_{V,i}\Psi+a_{V,i}\right)}\right)^2}\right\}\end{array}\right]. \quad (3)$$

The mean square error based objective/fitness formulation is formulated as follows:

$$E_{Fit} = E_{Fit-1} + E_{Fit-2} + E_{Fit-3}, \quad \textbf{(4)}$$

$$E_{Fit-1} = \frac{1}{N}\sum_{m=1}^{N}\left(\Psi_m \frac{d^2\hat{U}}{d\Psi_m^2} + \alpha \frac{d\hat{U}}{d\Psi_m} + \Psi_m H_1 G_1(\hat{U},\hat{V}) - \Psi_m F_1 \right)^2, \quad \textbf{(5)}$$

$$E_{Fit-2} = \frac{1}{N}\sum_{m=1}^{N}\left(\Psi_m \frac{d^2\hat{V}}{d\Psi_m^2} + \beta \frac{d\hat{V}}{d\Psi_m} + \Psi_m H_2 G_2(\hat{U},\hat{V}) - \Psi_m F_2 \right)^2, \quad \textbf{(6)}$$

$$E_{Fit-3} = \frac{1}{6}\left(\left(\hat{U} - A_1\right)^2 + \left(\frac{d\hat{U}}{d\Psi_m} \right)^2 + \left(\hat{V} - A_2\right)^2 + \left(\frac{d\hat{V}}{d\Psi_m} \right)^2 \right), \quad \textbf{(7)}$$

where $hN = 1$, $\Psi_m = mh$, $F_1(\Psi) = F_1$ and $F_2(\Psi) = F_2$. The objective functions E_{Fit-1} and E_{Fit-2} are linked with coupled differential systems and E_{Fit-3} is used for the initial conditions.

2.2 Optimization: PSO-IPM

The optimization to solve the second order nonlinear-coupled EF system is ratified by the hybrid-computing of PSO-IPM.

PSO is a well-organized search algorithm used as a global search methodology like genetic algorithms (GAs). The PSO algorithm introduced by Eberhart and Kennedy [55-56] and works as an easy procedure that needs minor memory. In search space, an applicant single solution of decision variables by applying optimization is known as a particle and these particles set formulate a swarm. The PSO operates via local $\boldsymbol{P}_{LB}^{\rho-1}$ and global $\boldsymbol{P}_{GB}^{\rho-1}$ best particle positions in a swarm. The position $\mathbf{X}_i$ and velocity $\boldsymbol{V}_i$ are mathematical expressed as follows:

$$\boldsymbol{X}_i^{\chi} = \boldsymbol{V}_i^{\chi-1} + \boldsymbol{X}_i^{\chi-1}, \quad \textbf{(8)}$$

$$\boldsymbol{V}_i^{\chi} = \sigma \boldsymbol{V}_i^{\chi-1} + \xi_1(\boldsymbol{P}_{LB}^{\chi-1} - \boldsymbol{X}_i^{\chi-1})\boldsymbol{\gamma}_1 + \xi_2(\boldsymbol{P}_{GB}^{\chi-1} - \boldsymbol{X}_i^{\chi-1})\boldsymbol{\gamma}_2, \quad \textbf{(9)}$$

here χ is stand for iteration/flight index, σ is for inertia weight vector varying between [0. 1], ξ_1 and ξ_2 are the cognitive/social constant accelerations, while, γ_1 and γ_2 are the vectors lie between [0, 1]. Some recent applications of PSO are parameter estimation [57], robotics [58-59], nonlinear electric circuits [60], systems of equations based physical models [61], and optimization of permanent magnets synchronous motor [62].

The convergence performance of PSO quickly achieved by using the combination with local search procedure by taking the global best particle of PSO as an initial weight. Consequently, an operative and quick local search approach named as interior-point method (IPM) is oppressed for rapid refinement of the outcomes obtained via PSO scheme. The integrated heuristics of PSO-IPM is exploited to train the networks, while the essential parameter settings of importance elements for

PSO-IPM is given in Table 1. Few recently IP scheme applications are power flow security constraint optimization [63], image processing [64], multistage nonlinear nonconvex problems [65] and nonlinear benchmark models [66]. The PSO-IP scheme is used to train the networks as per process and parameter settings provided in the Table 1.

Table 1: Comprehensive pseudocode of PSO-IP scheme for solving the second order nonlinear coupled EF model

PSO algorithm start
Step 1: Initialization: Create the prime swarm arbitrarily and initialize the parameters of PSO routine and optimoptions tool.
Step-2: Fitness Assessment: Determine/Analyze the fitness of each particle in the swarm using equations (4) to (7).
Step-3: Rank of particle: Ranking is associated for each particle of swarm via minimum criteria of the fitness/objrctive function.
Step-4: Stoppage Criteria: Terminate, if one of below standard meets

- Fitness level
- Selected flights

When the above standard accomplished, then go to Step 5
Step-5: Modification: Update the position and velocity by using expressions (8) and (9), respectively.
Step-6: Repetition: Repeat steps 2 to 6 till the whole flights are completed.
Step-7: Storage: The parameters of global best particle are store along with its fitness.
PSO algorithm stop
Start of PSO-IP scheme
Inputs: 'global best particle' of PSO
Output: $\mathbf{W}_{\mathbf{PSOIP}}$ are the 'PSOIP's trained weights
Initialization: Use 'global best particle' as a start point of IPM.
Termination: Stop the execution, when one of the below conditions meet
[Fitness = $E_{Fit} = 10^{-20}$], [TolX = 10^{-21}], [Generation = 1000], [TolFun = TolCon = 10^{-22}] and [MaxFunEvals = 265000]
While [Terminate]
Fitness Evaluation: The set (4) is applied for the 'fitness value'
Adjustments: Invoke the 'fmincon' routine for the IP scheme to regulate the 'weight vector' values.
Store the 'fitness values' using the 'basic form' of the 'weight vector'
Store: $\mathbf{W}_{\mathbf{PSO-IP}}$ scheme values, best weights, fitness, function count, generations and time for the current run.
PSO-IP scheme End

3. Performance indices/metrics

The performances is measured using RMSE, VAF, TIC indices along their globals, i.e., mean values. The mathematical forms of these statistical operatives are given as:

$$\left[RMSE_U, RMSE_V\right] = \left[\sqrt{\frac{1}{n}\sum_{k=1}^{n}\left(U_k - \hat{U}_k\right)^2}, \sqrt{\frac{1}{n}\sum_{k=1}^{n}\left(V_k - \hat{V}_k\right)^2}\right], \quad \textbf{(10)}$$

$$[\mathrm{TIC}_U,\mathrm{TIC}_V]=\left[\frac{\sqrt{\frac{1}{n}\sum_{k=1}^{n}\left(U(\Psi_k)-\hat{U}(\Psi_k)\right)^2}}{\left(\sqrt{\frac{1}{n}\sum_{k=1}^{n}U^2(\Psi_k)}+\sqrt{\frac{1}{n}\sum_{k=1}^{n}\hat{U}^2(\Psi_k)}\right)},\frac{\sqrt{\frac{1}{n}\sum_{k=1}^{n}\left(V(\Psi_k)-\hat{V}(\Psi_k)\right)^2}}{\left(\sqrt{\frac{1}{n}\sum_{k=1}^{n}V^2(\Psi_k)}+\sqrt{\frac{1}{n}\sum_{k=1}^{n}\hat{V}^2(\Psi_k)}\right)}\right], \tag{11}$$

$$\begin{cases}[VAF_U,VAF_V]=\left[\left(1-\frac{\mathrm{var}\left(U(\Psi_k)-\hat{U}(\Psi_k)\right)}{\mathrm{var}\left(U(\Psi_k)\right)}\right)\times 100,\left(1-\frac{\mathrm{var}\left(V(\Psi_k)-\hat{V}(\Psi_k)\right)}{\mathrm{var}\left(V(\Psi_k)\right)}\right)\times 100\right], \\ \left[EVAF_U,EVAF_V\right]=\left[\left|VAF_U-100\right|,\left|VAF_V-100\right|\right].\end{cases} \tag{12}$$

4. Results and discussions

The detail for presenting the solving the four examples of second order coupled EF model is presented in this section.

Problem I: Consider the second order nonlinear-coupled EF model is given as:

$$\begin{cases}\frac{d^2U}{d\Psi^2}+\frac{1}{\Psi}\frac{dU}{d\Psi}-(4\Psi^2+5)U=0,\ \ U(0)=1,\ \frac{dU(0)}{d\Psi}=0, \\ \frac{d^2V}{d\Psi^2}+\frac{2}{\Psi}\frac{dV}{d\Psi}-(4\Psi^2-5)V=0,\ \ \ V(0)=1,\ \frac{dV(0)}{d\Psi}=0.\end{cases} \tag{13}$$

The exact solutions of the equation (13) are [e^{Ψ^2}, $e^{-\Psi^2}$], whereas the fitness function becomes as:

$$E_{Fit}=\frac{1}{N}\sum_{m=0}^{N}\left(\begin{array}{l}\left(\Psi_m\frac{d^2\hat{U}}{d\Psi_m^2}+\frac{d\hat{U}}{d\Psi_m}-\Psi_m(4\Psi_m^2+5)\hat{U}\right)^2+ \\ \left(\Psi_m\frac{d^2\hat{V}}{d\Psi_m^2}+2\frac{d\hat{V}}{d\Psi_m}-\Psi_m(4\Psi_m^2-5)\hat{V}\right)^2\end{array}\right)+\frac{1}{4}\left(\begin{array}{l}\left(\hat{U}-1\right)^2+\left(\frac{d\hat{U}}{d\Psi_m}\right)^2 \\ +\left(\hat{V}-1\right)^2+\left(\frac{d\hat{V}}{d\Psi_m}\right)^2\end{array}\right), \tag{14}$$

here N =20, 25 and 30 for input span [0, 1], [0, 1.25] and [0, 1.5], respectively.

Problem II: Consider the second order nonlinear-coupled EF system is written as:

$$\begin{cases}\frac{d^2U}{d\Psi^2}+\frac{2}{\Psi}\frac{dU}{d\Psi}-U^2+V^2+6V=6\Psi^2+6,\ \ U(0)=1,\ \frac{dU(0)}{d\Psi}=0, \\ \frac{d^2V}{d\Psi^2}+\frac{2}{\Psi}\frac{dV}{d\Psi}+U^2-V^2-6V=-6\Psi^2+6,\ \ \ V(0)=-1,\ \frac{dV(0)}{d\Psi}=0.\end{cases} \tag{15}$$

The exact solutions of equation (15) are [$\Psi^2+e^{\Psi^2}$, $\Psi^2-e^{\Psi^2}$] and the error function is given as:

$$E_{Fit}=\frac{1}{N}\sum_{m=0}^{N}\left(\begin{array}{l}\left(\Psi_m\dfrac{d^2\hat{U}}{d\Psi_m^2}+2\dfrac{d\hat{U}}{d\Psi_m}-\Psi_m\hat{U}^2+\Psi_m\hat{V}^2+6\Psi_m\hat{V}=6\Psi_m^3+6\Psi_m\right)^2+\\ \left(\Psi_m\dfrac{d^2\hat{V}}{d\Psi_m^2}+2\dfrac{d\hat{V}}{d\Psi_m}+\Psi_m\hat{U}^2-\Psi_m\hat{V}^2-6\Psi_m\hat{V}=-6\Psi_m^3+6\Psi_m\right)^2\end{array}\right) \quad \textbf{(16)}$$
$$+\frac{1}{4}\left(\left(\hat{U}-1\right)^2+\left(\frac{d\hat{U}}{d\Psi_m}\right)^2+\left(\hat{V}+1\right)^2+\left(\frac{d\hat{V}}{d\Psi_m}\right)^2\right),$$

here N =20, 25 and 30 for input span [0, 1], [0, 1.25] and [0, 1.5], respectively.

Problem III: Consider the second order nonlinear-coupled EF model is given as:

$$\begin{cases}\dfrac{d^2U}{d\Psi^2}+\dfrac{3}{\Psi}\dfrac{dU}{d\Psi}-4(U+V)=0,\ \ U(0)=1,\ \dfrac{dU(0)}{d\Psi}=0,\\ \dfrac{d^2V}{d\Psi^2}+\dfrac{2}{\Psi}\dfrac{dV}{d\Psi}+3(U+V)=0,\ \ \ V(0)=1,\ \dfrac{dV(0)}{d\Psi}=0.\end{cases} \quad \textbf{(17)}$$

The exact solutions of the equation (17) are $[1+\Psi^2, 1-\Psi^2]$ and the fitness/objective function is given as follows:

$$E_{Fit}=\frac{1}{N}\sum_{m=0}^{N}\left(\begin{array}{l}\left(\Psi_m\dfrac{d^2\hat{U}}{d\Psi_m^2}+3\dfrac{d\hat{U}}{d\Psi_m}-4\Psi_m(\hat{U}+\hat{V})\right)^2+\\ \left(\Psi_m\dfrac{d^2\hat{V}}{d\Psi_m^2}+2\dfrac{d\hat{V}}{d\Psi_m}+3\Psi_m(\hat{U}+\hat{V})\right)^2\end{array}\right)+\frac{1}{4}\left(\begin{array}{l}\left(\hat{U}-1\right)^2+\left(\dfrac{d\hat{U}}{d\Psi_m}\right)^2\\ +\left(\hat{V}-1\right)^2+\left(\dfrac{d\hat{V}}{d\Psi_m}\right)^2\end{array}\right). \quad \textbf{(18)}$$

here N =20, 25 and 30 for input span [0, 1], [0, 1.25] and [0, 1.5], respectively.

Problem IV: Consider the second order nonlinear-coupled EF model is given as:

$$\begin{cases}\dfrac{d^2U}{d\Psi^2}+\dfrac{1}{\Psi}\dfrac{dU}{d\Psi}-(1+U^2)V^3=0,\ \ U(0)=1,\ \dfrac{dU(0)}{d\Psi}=0,\\ \dfrac{d^2V}{d\Psi^2}+\dfrac{3}{\Psi}\dfrac{dV}{d\Psi}+(3+U^2)V^5=0,\ \ \ V(0)=1,\ \dfrac{dV(0)}{d\Psi}=0.\end{cases} \quad \textbf{(19)}$$

The exact solutions of the equation (17) are $[\sqrt{1+\Psi^2}, \dfrac{1}{\sqrt{1+\Psi^2}}]$ and the fitness/objective function is given as follows:

$$E_{Fit}=\frac{1}{N}\sum_{m=0}^{N}\left(\begin{array}{l}\left(\Psi_m\frac{d^2\hat{U}}{d\Psi_m^2}+\frac{d\hat{U}}{d\Psi_m}-\hat{V}^3\Psi_m(\hat{U}^2+1)\right)^2+\\ \left(\Psi_m\frac{d^2\hat{V}}{d\Psi_m^2}+3\frac{d\hat{V}}{d\Psi_m}+\hat{V}^5\Psi_m(\hat{U}^2+3)\right)^2\end{array}\right)+\frac{1}{4}\left(\begin{array}{l}\left(\hat{U}-1\right)^2+\left(\frac{d\hat{U}}{d\Psi_m}\right)^2\\ +\left(\hat{V}-1\right)^2+\left(\frac{d\hat{V}}{d\Psi_m}\right)^2\end{array}\right), \quad \textbf{(20)}$$

here N =20, 25 and 30 for input span [0, 1], [0, 1.25] and [0, 1.5], respectively.

To calculate/determined the proposed numerical outcomes for the Problems I to IV based on the second order nonlinear-coupled EF model using the proposed PSO-IPM executed for 50 multiple runs to attain the adjustable weights. The numerical values of the weights are presented in Fig. 1 for $\hat{U}$ and $\hat{V}$ .. These parameters are applied to get the estimated results for all four variants based on the second order nonlinear-coupled EF model and the mathematical representations becomes as:

$$\hat{U}_{P-I}=\frac{1.6758}{1+e^{-(1.425\Psi+1.998)}}-\frac{3.8309}{1+e^{-(-4.376\Psi+5.970)}}+\frac{2.3451}{1+e^{-(1.5452\Psi-3.003)}}+\ldots-\frac{6.8234}{1+e^{-(-7.387\Psi+11.211)}}, \quad \textbf{(21)}$$

$$\hat{U}_{P-II}=\frac{6.0315}{1+e^{-(0.578\Psi+0.192)}}+\frac{9.0343}{1+e^{-(6.155\Psi-9.503)}}+\frac{1.297}{1+e^{-(-2.206\Psi-1.560)}}+\ldots+\frac{4.6126}{1+e^{-(-2.220\Psi-1.921)}}, \quad \textbf{(22)}$$

$$\hat{U}_{P-III}=\frac{-6.8663}{1+e^{-(-1.574\Psi+3.654)}}-\frac{1.0189}{1+e^{-(-0.492\Psi-1.299)}}-\frac{2.1697}{1+e^{-(-0.194\Psi-4.339)}}+\ldots+\frac{2.6387}{1+e^{-(-0.331\Psi+2.246)}}, \quad \textbf{(23)}$$

$$\hat{U}_{P-IV}=\frac{-0.2821}{1+e^{-(-0.533\Psi+2.368)}}+\frac{0.3969}{1+e^{-(2.391\Psi+1.929)}}-\frac{3.3036}{1+e^{-(-0.038\Psi-3.927)}}+\ldots-\frac{2.1545}{1+e^{-(-2.484\Psi-2.701)}}, \quad \textbf{(24)}$$

$$\hat{V}_{P-I}=\frac{-4.3366}{1+e^{-(-1.990\Psi-0.338)}}+\frac{4.8079}{1+e^{-(-0.598\Psi-3.336)}}-\frac{2.9912}{1+e^{-(0.600\Psi+2.518)}}+\ldots+\frac{1.1862}{1+e^{-(2.928\Psi+1.879)}}, \quad \textbf{(25)}$$

$$\hat{V}_{P-II}=\frac{-1.2095}{1+e^{-(1.812\Psi-1.701)}}-\frac{1.4677}{1+e^{-(-3.875\Psi-2.842)}}-\frac{5.4743}{1+e^{-(-0.276\Psi+2.736)}}+\ldots-\frac{4.5921}{1+e^{-(1.927\Psi+2.108)}}, \quad \textbf{(26)}$$

$$\hat{V}_{P-III}=\frac{2.237}{1+e^{-(0.454\Psi-0.035)}}-\frac{0.825}{1+e^{-(1.564\Psi+0.541)}}-\frac{0.249}{1+e^{-(1.204\Psi-0.301)}}+\ldots-\frac{0.7721}{1+e^{-(-1.792\Psi+0.440)}}, \quad \textbf{(27)}$$

$$\hat{V}_{P-IV}=\frac{-0.6548}{1+e^{-(2.202\Psi+2.856)}}+\frac{3.6090}{1+e^{-(5.003\Psi+2.080)}}-\frac{1.4197}{1+e^{-(5.548\Psi+1.859)}}+\ldots+\frac{3.1940}{1+e^{-(-0.815+2.385)}}. \quad \textbf{(28)}$$

The optimization is performed for all the problems of the nonlinear-coupled EF system with ANNs-PSO-IPM for 50 independent runs. A set of the best weights along with proposed and exact outcomes are shown in Fig.1. It is stated that all the problems of the nonlinear-coupled EF system of second kind, the exact/reference solution and ANNs-PSO-IPM results overlapped consistently for $\hat{U}(\Psi)$ and $\hat{V}(\Psi)$. This overlapping of the outcomes depicts the correctness/exactness of the

proposed ANNs-PSO-IP scheme. Fig 2 shows the absolute error (AE), comparison of the proposed results and exact solutions as well as analysis on different performance metrics. The approximate solutions for N = 25 and N = 30 are plotted in Fig. 3 and 4 along with the reference exact values. One may see that results are consistently overlapping for small as well as large interval. The AE plots for $\hat{U}(\Psi)$ and $\hat{V}(\Psi)$ are drawn in Figs 2(a) and 2(b) for N = 20, while the performance measures for $\hat{U}(\Psi)$ and $\hat{V}(\Psi)$ are provided in Figs 2(c) to 2(d) for N = 20. It is observed that the AE values of $\hat{U}(\Psi)$ lie around 10^{-05} to 10^{-06}, 10^{-04} to 10^{-05}, 10^{-06} to 10^{-08} and 10^{-06} to 10^{-07} for Problem I, II, III and IV in case of N = 20, 25 and 30. While the AE values of $\hat{V}(\Psi)$ lie around 10^{-05} to 10^{-06}, 10^{-04} to 10^{-05}, 10^{-06} to 10^{-09} and 10^{-06} to 10^{-07} for Problems I, II, III and IV for N = 20. The performance measures of $\hat{U}(\chi)$ and $\hat{V}(\Psi)$ based on FIT, RMSE, TIIC and EVAF are plotted in Fig. 2(c) and 2(d). It is seen that the FIT for $\hat{U}(\Psi)$ and $\hat{V}(\Psi)$ lie close to 10^{-08} to 10^{-10}, for problems I, III and IV, and similarly the FIT for Problem II lie around 10^{-06} to 10^{-08}. The RMSE and TIC for $\hat{U}(\Psi)$ and $\hat{V}(\Psi)$ lie around to 10^{-04} to 10^{-06}, for all the problems. The TIC values lie around 10^{-06} to 10^{-08} for both indexes of all the Problems. The values of the EVAF for both indices of all the problems lie around 10^{-10} to 10^{-12}. The convergence measures for the Problems I to IV based on the second order nonlinear-coupled EF model using the fitness values, boxplots and histograms with 10 neurons are plotted in Fig 5. It is seen that the fitness lie around 10^{-04} to 10^{-08} for the Problems I to IV.

For more satisfaction, accuracy and precision examination of the ANNs-PSO-IP scheme, statistical measures are made based on minimum (MIN), mean, standard deviation (SD), median and semi interquartile range (S-IR). S-IR range is 0.5 times of the difference of the third quartile i.e., Q_3=75% data and first quartile i.e., Q_1=25% data, is calculated for 50 runs of ANNs-PSO-IP scheme to solve four different examples of the nonlinear-coupled EF system of second kind. These statistical results for Problems I to IV are provided in Tables 2 as well as 3 for $\hat{U}$ and $\hat{V}$, respectively. It is perceived that both $\hat{U}(\Psi)$ and $\hat{V}(\Psi)$ for Problems I to IV lie in the good range. The global performance, i.e., G-FIT, G-EVAF, G-RMSE and G-TIC of $\hat{U}(\Psi)$ and $\hat{V}(\Psi)$ for Problems I to IV are provided in Table 4. In the said Table, the presentations of the global performance for all problems based on second order nonlinear-coupled EF model for 50 independent executions are provided. The magnitude as well as median values of each Problems based on the second order nonlinear-coupled EF model using the indexes $\hat{U}(\Psi)$ and $\hat{V}(\Psi)$ proven good. The time complexity of the proposed scheme ANNs-PSO-IPM for all four problems in terms of time consume for learning of weights of neural network is around 50±25 for N = 20, while in case of N =25 and 30 time consumed are around 55±25 and 60±20, respectively.

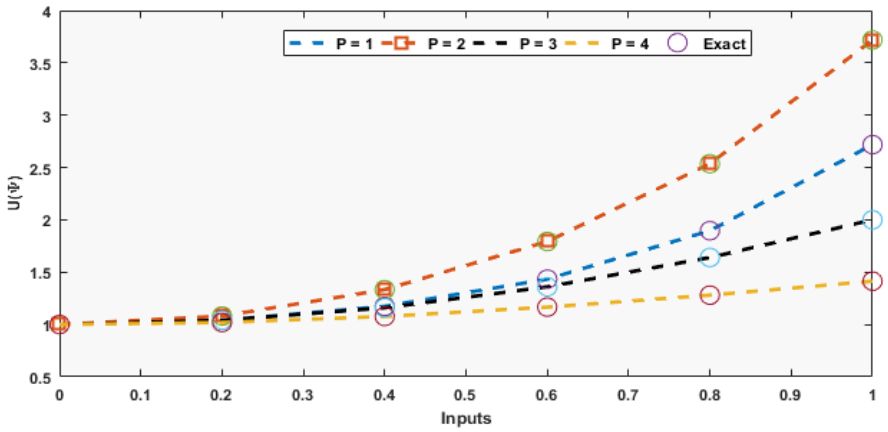

(a): Results of $\hat{U}(\Psi)$ for Problems I to IV

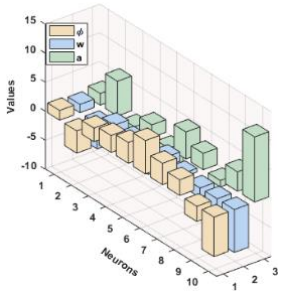

(b): P-I weights for $\hat{U}(\Psi)$

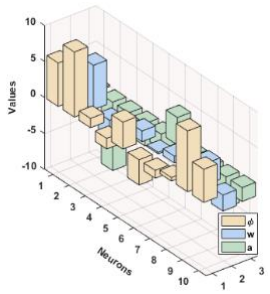

(c): P-II weights for $\hat{U}(\Psi)$

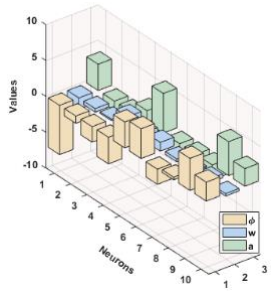

(d): P-III weights for $\hat{U}(\Psi)$

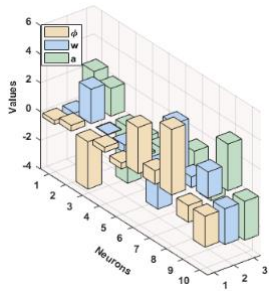

(e): P-IV weights for $\hat{U}(\Psi)$

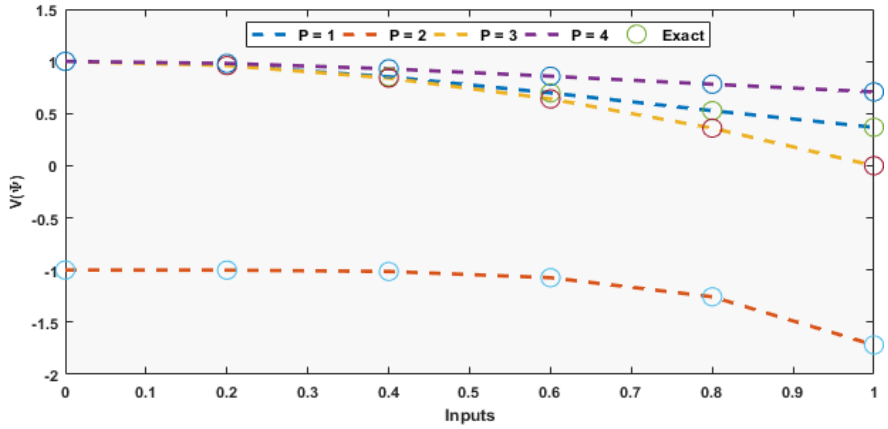

(f): Results of $\hat{V}(\Psi)$ for Problems I to IV

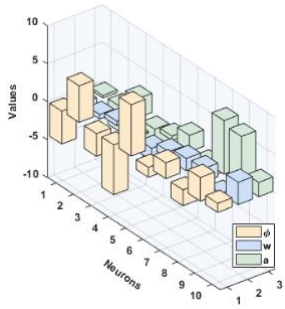

(g): P-I weights for $\hat{V}(\Psi)$

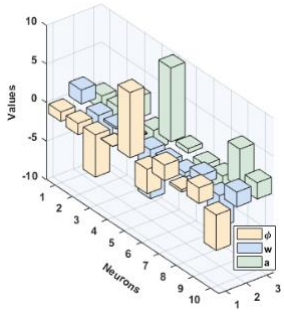

(h): P-II weights for $\hat{V}(\Psi)$

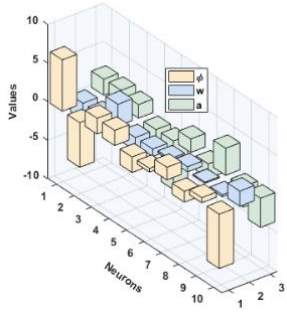

(i): P-III weights for $\hat{V}(\Psi)$

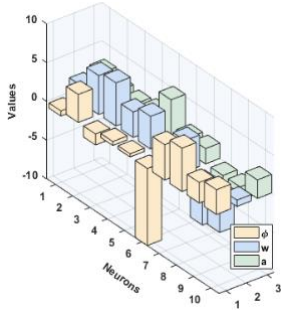

(j): P-IV weights for $\hat{V}(\Psi)$

Fig 1: Best weight sets and results comparison for all the Problems of second order nonlinear-coupled EF model

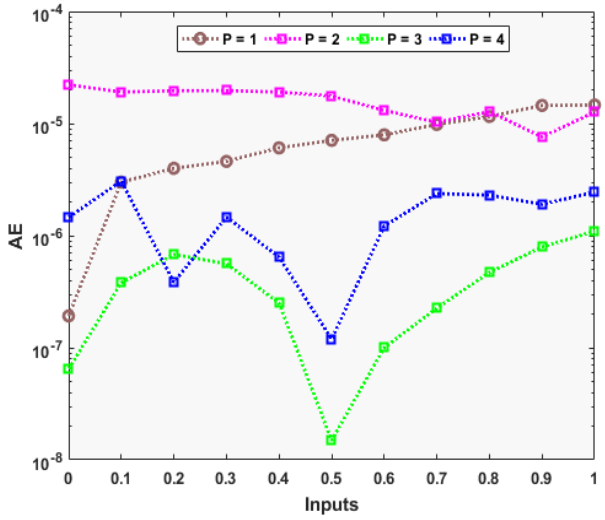

(a) AE of Problems I-IV for $\hat{U}(\Psi)$

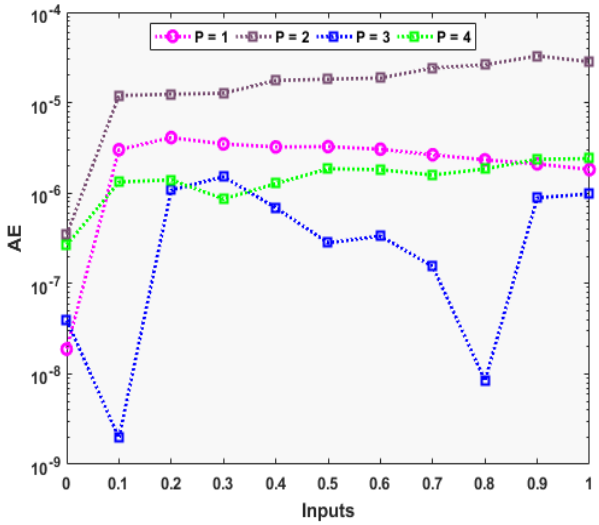

(b) AE of Problems I-IV for $\hat{V}(\Psi)$

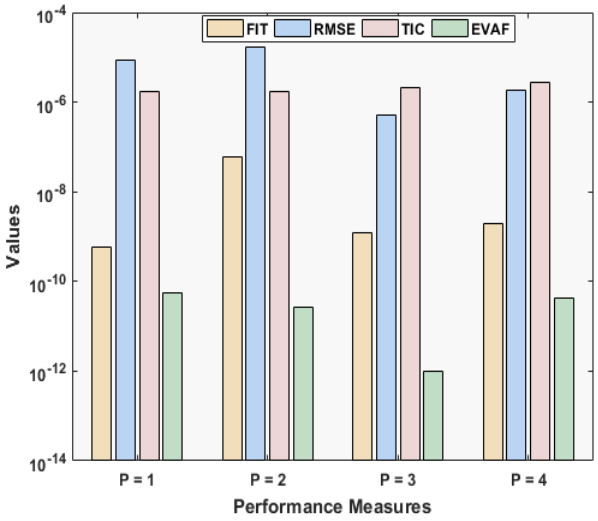

(c) Performance indices of Problem I-IV for $\hat{U}(\Psi)$

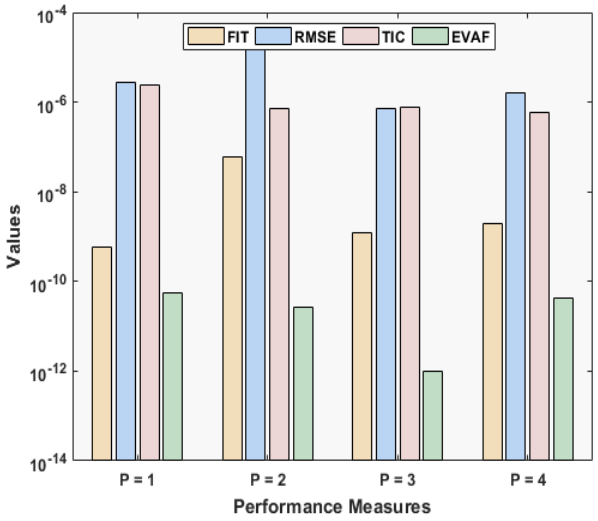

(d) Performance indices of Problem I-IV for $\hat{V}(\Psi)$

Fig 2: Absolute error and performance measures for all Problems of second order nonlinear-coupled EF model.

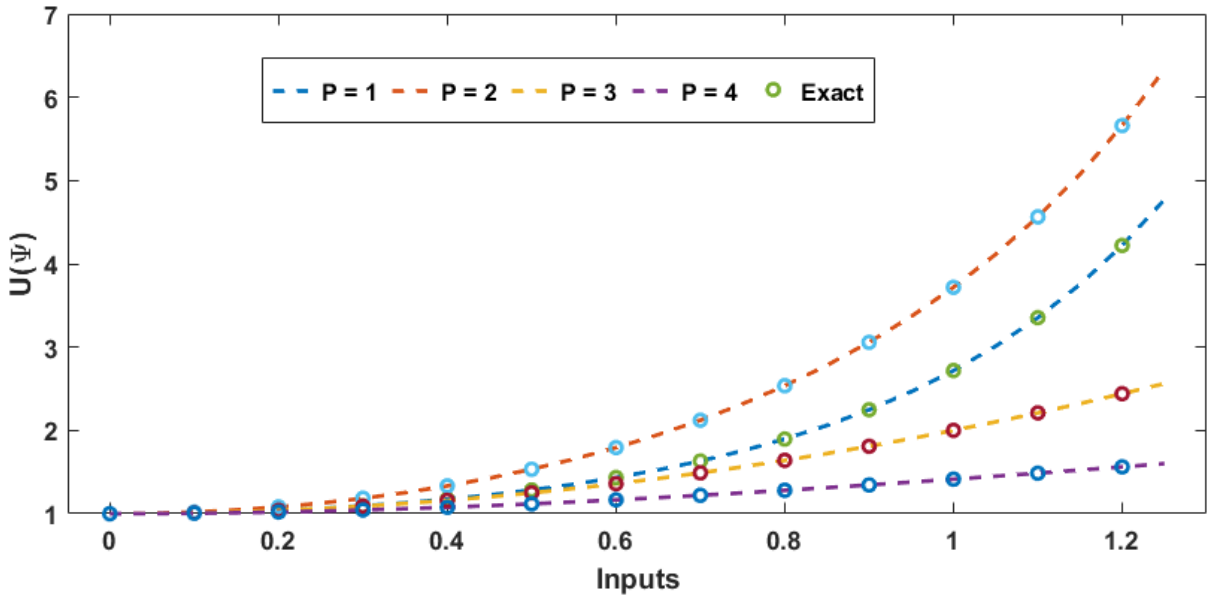

(a) results for U(Ψ)

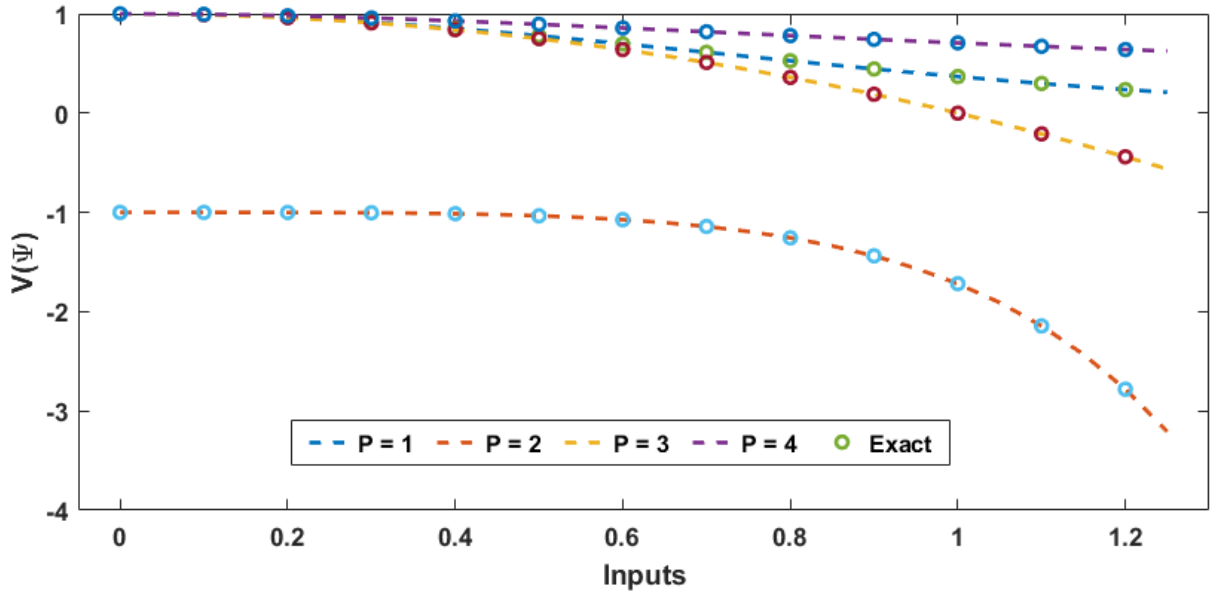

(a) results for V(Ψ)

Fig 3: Comparison of proposed solutions for all Problems of second order nonlinear-coupled EF model in case of input interval [0, 1.25].

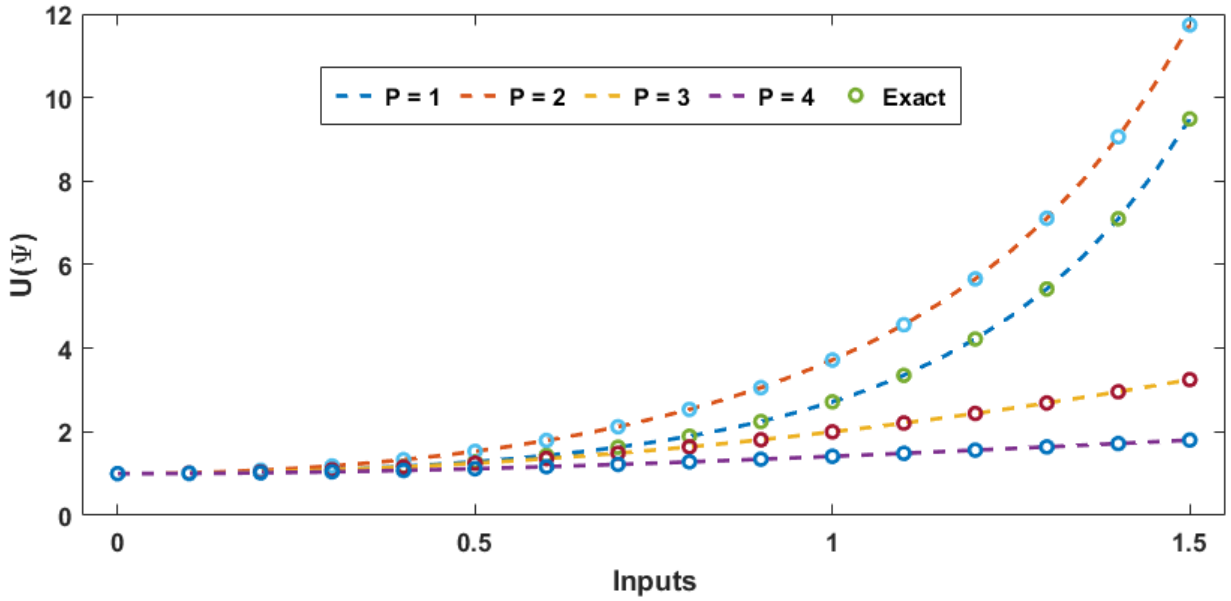

(a) results for U(Ψ)

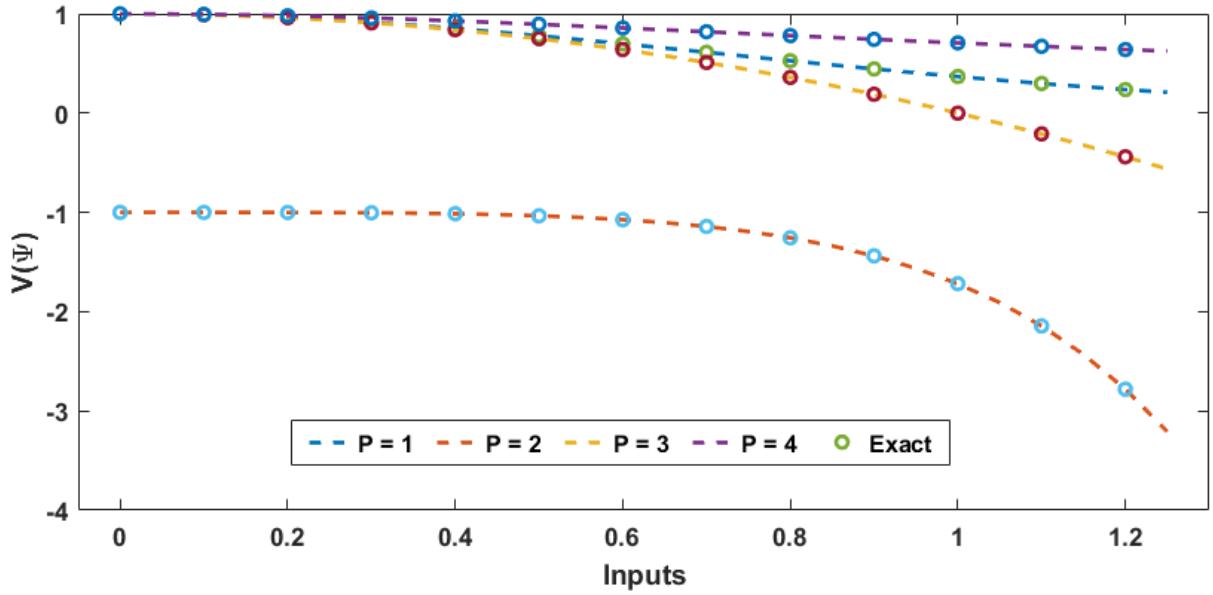

(b) results for V(Ψ)

Fig 4: Comparison of proposed solutions for all Problems of second order nonlinear-coupled EF model in case of input interval [0, 1.5].

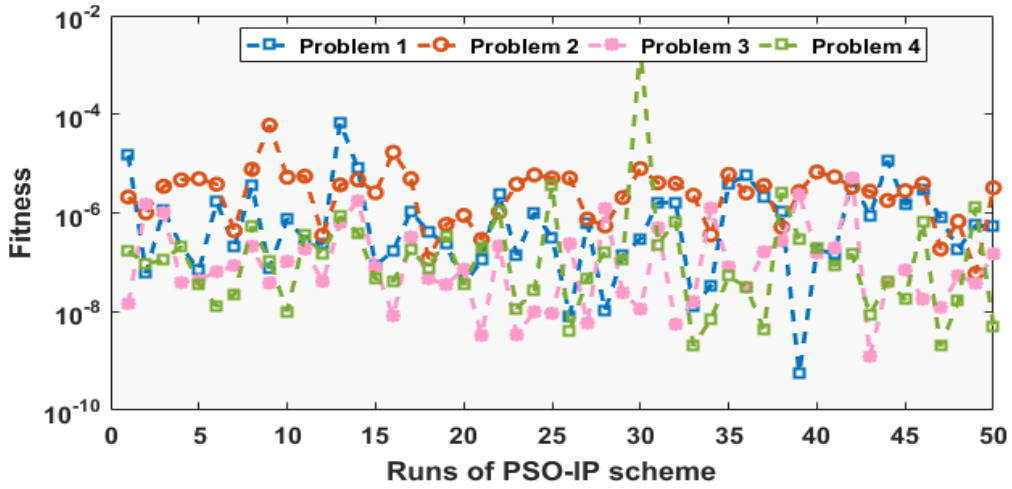

(a) Convergence analysis of second order nonlinear-coupled EF model based on the independent trials ANNs-PSO-IP scheme along x-axis and Fitness values on y-axis

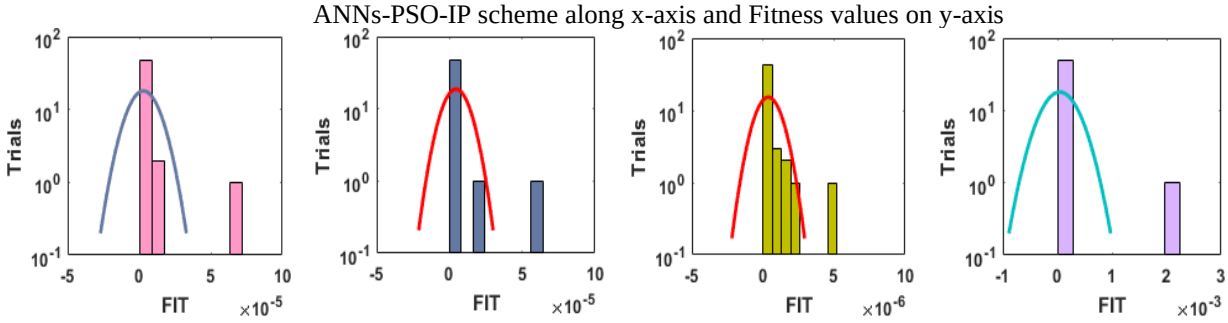

(b): Histogram for Problem I

(c): Histogram for Problem II

(d): Histogram for Problem III

(e): Histogram for Problem IV

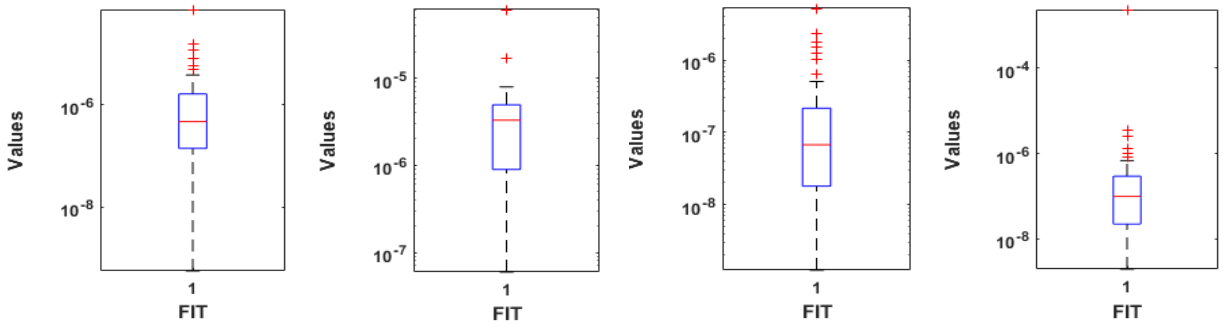

(f): Boxplot for Problem I

(g): Boxplot for Problem II

(h): Boxplot for Problem III

(i): Boxplot for Problem IV

Fig 5: Convergence indices for all the Problems of second order nonlinear-coupled EF model using the Fitness, boxplots and boxplots for 10 neurons

Table 2: Statistics on $\hat{U}(\Psi)$ for all the Problems of second order nonlinear-coupled EF model using the ANNs-PSO-IP approach.

	Mode	Solutions of $\hat{U}(\Psi)$ for Problems I to IV between [0,1]										
		0	**0.10**	**0.20**	**0.30**	**0.40**	**0.50**	**0.60**	**0.70**	**0.80**	**0.90**	**1.0**
Problem I	Min	3.5×10-07	3.0×10-06	4.0×10-06	4.6×10-06	6.1×10-06	7.0×10-06	7.9×10-06	9.8×10-06	1.2×10-05	1.5×10-05	1.5×10-05
	Mean	4.9×10-05	5.7×10-03	8.5×10-03	2.2×10-02	2.4×10-02	2.6×10-02	1.9×10-02	4.7×10-02	3.8×10-02	3.1×10-02	4.9×10-02
	SD	2.7×10-04	1.8×10-02	2.4×10-02	5.0×10-02	6.9×10-02	7.9×10-02	6.8×10-02	5.5×10-02	6.5×10-02	7.8×10-01	9.4×10-01
	Median	3.4×10-07	7.5×10-04	2.4×10-03	2.5×10-03	5.9×10-05	3.5×10-03	9.7×10-04	8.1×10-05	3.2×10-06	8.2×10-05	1.9×10-05
	SIR	1.7×10-05	8.3×10-05	6.4×10-05	3.5×10-04	2.4×10-06	2.6×10-05	2.4×10-04	3.5×10-04	7.4×10-05	1.9×10-05	6.5×10-04
Problem II	Min	7.5×10-07	1.3×10-06	4.5×10-05	9.7×10-05	2.0×10-07	1.5×10-07	3.3×10-07	1.0×10-05	2.6×10-06	7.8×10-06	2.6×10-07
	Mean	3.9×10-05	9.7×10-05	1.5×10-03	1.5×10-04	3.9×10-04	2.9×10-05	2.0×10-04	2.3×10-04	2.6×10-05	3.1×10-05	3.7×10-05
	SD	6.6×10-05	1.1×10-04	1.5×10-04	1.5×10-04	1.5×10-04	1.6×10-04	1.9×10-06	2.1×10-03	2.3×10-03	9.2×10-04	3.3×10-05
	Median	9.6×10-06	7.2×10-05	4.5×10-05	1.1×10-04	1.0×10-04	1.1×10-04	1.4×10-04	1.7×10-04	2.1×10-04	3.5×10-05	3.5×10-04
	SIR	1.8×10-05	4.7×10-05	2.3×10-06	8.7×10-05	7.2×10-05	7.9×10-06	9.8×10-06	9.5×10-05	1.0×10-02	9.2×10-04	1.9×10-05
Problem III	Min	1.1×10-08	7.6×10-07	7.8×10-07	6.1×10-07	5.7×10-08	2.6×10-08	2.1×10-07	3.3×10-07	5.6×10-07	5.6×10-07	4.4×10-07
	Mean	4.4×10-06	6.9×10-06	3.4×10-06	4.2×10-04	2.9×10-07	4.5×10-06	3.0×10-05	4.3×10-06	3.4×10-04	3.7×10-06	3.2×10-06
	SD	6.5×10-05	6.1×10-05	3.8×10-05	3.2×10-05	3.4×10-05	6.1×10-04	4.3×10-04	3.6×10-05	4.2×10-03	4.4×10-05	5.2×10-04
	Median	9.6×10-06	3.9×10-04	8.1×10-06	7.2×10-06	7.3×10-06	8.0×10-05	8.7×10-05	6.3×10-07	3.6×10-05	6.2×10-04	1.6×10-05
	SIR	2.9×10-06	8.4×10-06	9.5×10-04	9.2×10-07	4.3×10-06	7.3×10-06	4.5×10-07	2.1×10-05	9.1×10-06	3.3×10-07	1.7×10-06
Problem IV	Min	3.3×10-08	4.4×10-07	6.8×10-07	1.5×10-05	9.2×10-07	3.4×10-07	2.2×10-06	5.4×10-06	5.4×10-07	6.4×10-06	2.2×10-06
	Mean	6.5×10-04	1.0×10-02	2.7×10-05	5.1×10-03	3.4×10-03	2.7×10-04	1.2×10-04	6.1×10-05	2.4×10-03	3.6×10-04	3.6×10-04
	SD	7.4×10-03	9.3×10-03	4.2×10-03	3.5×10-03	2.6×10-02	2.6×10-03	3.4×10-03	5.2×10-03	4.6×10-02	2.5×10-03	2.6×10-03
	Median	4.9×10-06	2.5×10-05	6.2×10-05	5.8×10-05	4.3×10-05	5.4×10-05	5.9×10-06	6.7×10-04	6.0×10-05	8.4×10-04	6.8×10-05
	SIR	8.1×10-06	4.9×10-06	9.4×10-06	7.2×10-04	6.6×10-06	4.5×10-06	7.8×10-05	7.4×10-05	7.3×10-06	6.2×10-06	5.4×10-06

Table 3: Statistics on $\hat{V}(\Psi)$ for all Problems of second order nonlinear-coupled EF model using the ANNs-PSO-IP approach.

	Mode	Solutions of $\hat{V}(\Psi)$ for Problems I to IV between [0,1] with 0.1 step size										
		0	**0.1**	**0.2**	**0.3**	**0.4**	**0.5**	**0.6**	**0.7**	**0.8**	**0.9**	**1**
Problem I	Min	2.7×10-08	8.3×10-07	7.0×10-07	4.6×10-07	2.3×10-07	6.2×10-07	2.3×10-07	2.2×10-07	2.2×10-06	6.0×10-07	4.8×10-07
	Mean	3.2×10-06	7.3×10-05	4.2×10-04	2.2×10-03	3.2×10-03	3.5×10-03	5.2×10-03	6.7×10-03	8.8×10-03	2.2×10-03	2.3×10-04
	SD	8.4×10-04	2.4×10-04	7.4×10-04	3.6×10-03	5.3×10-03	8.7×10-03	2.3×10-03	2.7×10-03	3.3×10-03	3.7×10-03	3.2×10-03
	Median	7.3×10-05	2.7×10-05	3.7×10-05	3.6×10-05	2.7×10-05	2.4×10-05	2.5×10-05	2.8×10-05	2.4×10-05	2.4×10-05	2.5×10-06
	SIR	2.0×10-06	2.3×10-05	3.4×10-05	3.5×10-05	2.7×10-05	2.4×10-05	2.6×10-05	2.5×10-05	2.3×10-05	2.5×10-05	2.2×10-05
Problem II	Min	2.0×10-07	4.0×10-06	3.3×10-06	3.3×10-07	3.2×10-06	5.4×10-06	2.7×10-06	7.5×10-07	2.7×10-05	3.7×10-07	2.3×10-05
	Mean	3.0×10-05	2.0×10-04	2.8×10-04	3.0×10-04	2.7×10-04	3.0×10-04	3.3×10-04	3.6×10-04	3.7×10-04	3.4×10-04	3.7×10-05
	SD	3.7×10-05	7.7×10-05	2.4×10-04	2.5×10-04	2.4×10-04	2.5×10-04	2.7×10-04	2.7×10-04	3.2×10-04	3.6×10-04	3.0×10-04
	Median	3.2×10-05	2.0×10-04	2.5×10-04	2.5×10-04	2.6×10-04	2.8×10-04	3.2×10-04	3.6×10-04	3.7×10-04	3.5×10-04	3.7×10-04
	SIR	2.7×10-05	4.8×10-05	2.0×10-04	2.3×10-04	2.3×10-04	2.3×10-04	2.3×10-04	2.6×10-04	2.7×10-04	2.7×10-04	3.3×10-04
Problem III	Min	2.4×10-08	3.0×10-07	2.2×10-06	2.4×10-07	6.7×10-07	3.8×10-07	3.3×10-07	3.5×10-07	8.4×10-07	3.3×10-08	2.8×10-07
	Mean	7.7×10-06	2.6×10-05	3.5×10-05	3.4×10-05	3.0×10-05	2.8×10-05	2.8×10-05	2.8×10-05	2.6×10-05	2.4×10-05	2.4×10-06
	SD	2.3×10-05	2.7×10-05	3.8×10-05	3.7×10-05	3.4×10-05	3.0×10-05	2.7×10-05	4.7×10-05	2.7×10-05	2.7×10-05	2.6×10-05
	Median	3.8×10-06	8.8×10-06	2.5×10-05	2.3×10-05	2.2×10-05	2.2×10-05	2.2×10-05	2.0×10-05	7.6×10-06	8.2×10-06	7.3×10-06
	SIR	4.8×10-06	7.4×10-06	2.4×10-05	2.3×10-05	2.3×10-05	2.2×10-05	2.2×10-05	7.0×10-06	8.0×10-06	7.5×10-06	6.7×10-06
Problem IV	Min	7.2×10-08	3.7×10-08	2.8×10-07	4.5×10-07	3.3×10-07	2.2×10-06	6.0×10-07	3.4×10-08	2.3×10-07	3.3×10-07	3.3×10-07
	Median	7.4×10-04	7.3×10-04	6.3×10-04	4.7×10-04	3.7×10-04	4.5×10-05	3.2×10-04	4.3×10-04	6.3×10-04	7.7×10-04	7.4×10-04
	SD	5.2×10-03	4.7×10-03	4.3×10-03	3.3×10-03	2.8×10-03	3.3×10-04	2.4×10-03	3.7×10-03	4.3×10-03	5.6×10-03	6.6×10-03
	Median	4.8×10-06	2.2×10-05	2.7×10-05	2.4×10-05	8.2×10-06	8.3×10-06	8.3×10-06	7.7×10-06	3.6×10-06	3.8×10-06	4.4×10-06
	SIR	6.7×10-06	2.5×10-05	2.6×10-05	2.2×10-05	7.6×10-06	7.3×10-06	6.5×10-06	5.0×10-06	4.5×10-06	4.7×10-06	4.0×10-07

Table 4: Results for global performance on both $\hat{U}(\Psi)$ and $\hat{V}(\Psi)$ in case of Problems I to IV

Index	Problem	G.FIT		G.RMSE		G.TIC		G.EVAF	
		MAG	Median	MAG	Median	MAG	Median	MAG	Median
$\hat{U}(\Psi)$	1	2.95×10-06	4.71×10-07	2.06×10-01	2.28×10-04	2.77×10-02	4.16×10-05	2.71×10-01	4.20×10-08
	2	4.47×10-06	3.29×10-06	2.15×10-04	1.69×10-04	3.95×10-02	4.27×10-05	1.82×10-08	8.89×10-09
	3	3.73×10-07	6.71×10-08	2.26×10-05	1.01×10-05	5.41×10-02	5.44×10-05	1.80×10-09	1.43×10-10
	4	4.42×10-05	9.90×10-08	2.62×10-02	4.77×10-05	5.87×10-02	6.05×10-05	2.94×10-01	2.22×10-08
$\hat{V}(\Psi)$	1	6.6×10-06	3.1×10-07	6.3×10-05	4.2×10-06	1.9×10-05	9.1×10-07	3.6×10-08	5.8×10-09
	2	3.5×10-04	4.8×10-06	5.1×10-02	2.4×10-02	1.2×10-05	7.3×10-06	3.3×10-01	2.1×10-03
	3	1.7×10-06	3.1×10-07	1.8×10-05	8.1×10-06	1.7×10-05	1.1×10-05	3.2×10-09	9.5×10-11
	4	2.3×10-05	2.1×10-07	5.8×10-02	3.5×10-06	5.8×10-03	7.5×10-06	3.5×10-02	2.5×10-03

4. Conclusion

In this investigation, a reliable, stable, consistent and precise numerical ANNs-PSO-IPM is presented for solving the nonlinear-coupled EF system by using the ANNs strength. The objective function is optimized of these networks using the global as well as local search competences of PSO-IPM. The suggested ANNs-PSO-IPM is viably executed to solve four different examples of the nonlinear-coupled EF system. The detailed, precise and particular presentation is obtained for ANNs-PSO-IPM in terms of AE with steadfast precision is measured around 4 to 7 decimals of accurateness of the present reference solutions for all four problems of the nonlinear-coupled EF system of second kind. Furthermore, the statistical clarifications achieved good measures using the Min, standard deviation, Mean, S-IR and Median to check the convergence, robustness and accuracy of the ANNs-PSO-IPM for solving the second order nonlinear-coupled EF model based problems I to IV.

5. Future research directions

In the future, one can exploit/explore the knacks of ANNs-PSO-IPM to solve the singular higher order models [67-69], fractional order models [70-75] and many other applications of utmost importance [76-79].

References

[1] Burdyny, T., & Smith, W. A. (2019). CO 2 reduction on gas-diffusion electrodes and why catalytic performance must be assessed at commercially-relevant conditions. Energy & Environmental Science, 12(5), 1442-1453.

[2] Abbas, F., Kitanov, P., & Longo, S. (2019). Approximate solutions to lane-emden equation for stellar configuration. Appl. Math. Inf. Sci, 13, 143-152.

[3] Bacchini, C., Fraternali, F., Iorio, G., & Pezzulli, G. (2019). Volumetric star formation laws of disc galaxies. Astronomy & Astrophysics, 622, A64.

[4] Soliman, M.A., (2019). Approximate solution for the Lane-Emden equation of the second kind in a spherical annulus. *Journal of King Saud University-Engineering Sciences*, *31*(1), pp.1-5.

[5] Adel, W., & Sabir, Z. (2020). Solving a new design of nonlinear second-order Lane–Emden pantograph delay differential model via Bernoulli collocation method. The European Physical Journal Plus, 135(5), 1-12.

[6] Barilla, D., Caristi, G., Heidarkhani, S., & Moradi, S. (2020). Generalized yamabe equations on riemannian manifolds and applications to Emden-Fowler problems. Quaestiones Mathematicae, 43(4), 547-567.

[7] Guirao, J. L., Sabir, Z., & Saeed, T. (2020). Design and numerical solutions of a novel third-order nonlinear Emden–Fowler delay differential model. Mathematical Problems in Engineering, 2020.

[8] Dridi, A., & Trabelsi, N. (2022). Blow up solutions for a 4-dimensional Emden–Fowler system of Liouville type. Journal of Elliptic and Parabolic Equations, 1-36.

[9] Dizicheh, A. K., Salahshour, S., Ahmadian, A., & Baleanu, D. (2020). A novel algorithm based on the Legendre wavelets spectral technique for solving the Lane–Emden equations. Applied Numerical Mathematics, 153, 443-456.

[10] Abdullah Alderremy, A., Elzaki, T. M., & Chamekh, M. (2019). Modified Adomian decomposition method to solve generalized Emden–Fowler systems for singular IVP. Mathematical Problems in Engineering, 2019.

[11] Singh, R., Guleria, V. & Singh, M., (2020). Haar wavelet quasilinearization method for numerical solution of Emden–Fowler type equations. *Mathematics and Computers in Simulation*, *174*, pp.123-133.

[12] Verma, A. K., & Kumar, N. (2019). Haar wavelets collocation on a class of Emden-Fowler equation via Newton's quasilinearization and Newton-Raphson techniques. arXiv preprint arXiv:1911.05819.

[13] Arqub, O. A., Osman, M. S., Abdel-Aty, A. H., Mohamed, A. B. A., & Momani, S. (2020). A numerical algorithm for the solutions of ABC singular Lane–Emden type models arising in astrophysics using reproducing kernel discretization method. Mathematics, 8(6), 923..

[14] Dizicheh, A. K., Salahshour, S., Ahmadian, A., & Baleanu, D. (2020). A novel algorithm based on the Legendre wavelets spectral technique for solving the Lane–Emden equations. Applied Numerical Mathematics, 153, 443-456.

[15] Verma, A. K., Kumar, N., Singh, M., & Agarwal, R. P. (2021). A note on variation iteration method with an application on Lane–Emden equations. Engineering Computations..

[16] Xie, L.J., Zhou, C.L. & Xu, S., (2019). Solving the systems of equations of Lane-Emden type by differential transform method coupled with adomian polynomials. *Mathematics*, *7*(4), p.377.

[17] Roul, P. & Thula, K., (2019). A fourth-order B-spline collocation method and its error analysis for Bratu-type and Lane–Emden problems. *International Journal of Computer Mathematics*, *96*(1), pp.85-104.

[18] Sharma, B., Kumar, S., Paswan, M.K. & Mahato, D., (2019). Chebyshev Operational Matrix Method for Lane-Emden Problem. *Nonlinear Engineering*, *8*(1), pp.1-9.

[19] Khalifa, A.S. & Hassan, H.N., (2019). Approximate Solution of Lane-Emden Type Equations Using Variation of Parameters Method with an Auxiliary Parameter. *Journal of Applied Mathematics and Physics*, *7*(04), p.921.

[20] Alharbi, A.R., Almatrafi, M.B. & Lotfy, K., (2020). Constructions of solitary travelling wave solutions for Ito integro-differential equation arising in plasma physics. Results in Physics, 19, p.103533.

[21] Almatrafi, M.B., Alharbi, A., Lotfy, K. & El-Bary, A.A., (2021). Exact and numerical solutions for the GBBM equation using an adaptive moving mesh method. Alexandria Engineering Journal, 60(5), pp.4441-4450.

[22] Abdelrahman, M.A. & Alharbi, A., (2021). Analytical and numerical investigations of the modified Camassa–Holm equation. Pramana, 95(3), pp.1-9.

[23] Sabir, Z., Wahab, H. A., Nguyen, T. G., Altamirano, G. C., Erdoğan, F., & Ali, M. R. (2022). Intelligent computing technique for solving singular multi-pantograph delay differential equation. Soft Computing, 1-13.

[24] Sabir, Z. (2022). Neuron analysis through the swarming procedures for the singular two-point boundary value problems arising in the theory of thermal explosion. The European Physical Journal Plus, 137(5), 1-18.

[25] Lotfy, K., (2019). Effect of variable thermal conductivity during the photothermal diffusion process of semiconductor medium. Silicon, 11(4), pp.1863-1873.

[26] Sabir, Z., Raja, M. A. Z., Umar, M., & Shoaib, M. (2020). Neuro-swarm intelligent computing to solve the second-order singular functional differential model. The European Physical Journal Plus, 135(6), 1-19..

[27] Lu, K.D., Zeng, G.Q. & Zhou, W., (2021). Adaptive constrained population extremal optimisation-based robust proportional-integral-derivation frequency control method for an islanded microgrid. *IET Cyber-Systems and Robotics*, *3*(3), pp.210-227.

[28] Lu, K., Zhou, W., Zeng, G. & Zheng, Y. (2019). Constrained population extremal optimization-based robust load frequency control of multi-area interconnected power system. *International Journal of Electrical Power & Energy Systems*, *105*, pp.249-271.

[29] Sabir, Z., et al., (2020). Novel design of Morlet wavelet neural network for solving second order Lane–Emden equation. Mathematics and Computers in Simulation, 172, pp.1-14.

[30] Guerrero–Sánchez, Y., Umar, M., Sabir, Z., Guirao, J. L., & Raja, M. A. Z. (2021). Solving a class of biological HIV infection model of latently infected cells using heuristic approach. Discrete & Continuous Dynamical Systems-S, 14(10), 3611.

[31] Mehmood, A., et al., (2020). Integrated computational intelligent paradigm for nonlinear electric circuit models using neural networks, genetic algorithms and sequential quadratic programming. *Neural Computing and Applications*, *32*(14), pp.10337-10357.

[32] Guirao, J. L., Sabir, Z., Raja, M. A. Z., & Baleanu, D. (2022). Design of neuro-swarming computational solver for the fractional Bagley–Torvik mathematical model. The European Physical Journal Plus, 137(2), 245..

[33] Bukhari, A.H., et al., (2020). Fractional neuro-sequential ARFIMA-LSTM for financial market forecasting. *IEEE Access*, *8*, pp.71326-71338.

[34] Sabir, Z. (2022). Stochastic numerical investigations for nonlinear three-species food chain system. International Journal of Biomathematics, 15(04), 2250005.

[35] Saeed, T., et al. (2022). An advanced heuristic approach for a nonlinear mathematical based medical smoking model. Results in Physics, 32, 105137.

[36] Sabir, Z., et al., (2022). FMNSICS: Fractional Meyer neuro-swarm intelligent computing solver for nonlinear fractional Lane–Emden systems. *Neural Computing and Applications*, *34*(6), pp.4193-4206.

[37] Nisar, K., et al. (2021). Design of morlet wavelet neural network for solving a class of singular pantograph nonlinear differential models. IEEE Access, 9, 77845-77862.

[38] Mahmood, T., et al., (2022). Novel Adaptive Bayesian Regularization Networks for Peristaltic Motion of a Third-Grade Fluid in a Planar Channel. *Mathematics*, *10*(3), p.358.

[39] Umar, M., et al., (2019). Intelligent computing for numerical treatment of nonlinear prey–predator models. Applied Soft Computing, 80, 506-524.

[40] Fateh, M.F., et al., (2019). Differential evolution based computation intelligence solver for elliptic partial differential equations. Frontiers of Information Technology & Electronic Engineering, 20(10), pp.1445-1456.

[41] Botmart, T., et al. (2022). A hybrid swarming computing approach to solve the biological nonlinear Leptospirosis system. Biomedical Signal Processing and Control, 77, 103789.

[42] Sabir, Z., Umar, M., Raja, M. A. Z., & Baleanu, D. (2021). Numerical Solutions of a Novel Designed Prevention Class in the HIV Nonlinear Model. CMES-COMPUTER MODELING IN ENGINEERING & SCIENCES, 129(1), 227-251.

[43] Sabir, Z., Umar, M., Raja, M. A. Z., Baskonus, H. M., & Gao, W. (2022). Designing of Morlet wavelet as a neural network for a novel prevention category in the HIV system. International Journal of Biomathematics, 15(04), 2250012.

[44] Raja, M. A. Z., Mehmood, J., Sabir, Z., Nasab, A. K., and Manzar, M. A. (2019). Numerical solution of doubly singular nonlinear systems using neural networks-based integrated intelligent computing. Neural Computing and Applications, 31(3), 793-812.

[45] Sabir, Z., et al., (2018). Neuro-heuristics for nonlinear singular Thomas-Fermi systems. Applied Soft Computing, 65, 152-169.

[46] Malešević, N., Petrović, V., Belić, M., Antfolk, C., Mihajlović, V., & Janković, M. (2020). Contactless real-time heartbeat detection via 24 GHz continuous-wave Doppler radar using artificial neural networks. Sensors, 20(8), 2351..

[47] Wang, B., Gomez-Aguilar, J. F., Sabir, Z., Zahoor Raja, M. A., Xia, W. F., Jahanshahi, H., & Alsaadi, F. E. (2022). Numerical computing to solve the nonlinear corneal system of eye surgery using the capability of Morlet wavelet artificial neural networks. Fractals.

[48] Umar, M., Amin, F., Wahab, H.A. & Baleanu, D., (2019). Unsupervised constrained neural network modeling of boundary value corneal model for eye surgery. Applied Soft Computing, 85, p.105826.

[49] Raja, M. A. Z., Umar, M., Sabir, Z., Khan, J. A., & Baleanu, D. (2018). A new stochastic computing paradigm for the dynamics of nonlinear singular heat conduction model of the human head. The European Physical Journal Plus, 133(9), 364.

[50] Sabir, Z., Amin, F., Pohl, D. & Guirao, J.L., (2020). Intelligence computing approach for solving second order system of Emden–Fowler model. *Journal of Intelligent & Fuzzy Systems*, *38*(6), pp.7391-7406.

[51] Sabir, Z., Botmart, T., Raja, M. A. Z., Sadat, R., Ali, M. R., Alsulami, A. A., & Alghamdi, A. (2022). Artificial neural network scheme to solve the nonlinear influenza disease model. Biomedical Signal Processing and Control, 75, 103594.

[52] Sabir, Z., et al., (2021). Design of Gudermannian Neuroswarming to solve the singular Emden–Fowler nonlinear model numerically. *Nonlinear Dynamics*, *106*(4), pp.3199-3214.

[53] Nasirzadehroshenin, F., Sadeghzadeh, M., Khadang, A., Maddah, H., Ahmadi, M.H., Sakhaeinia, H. & Chen, L., (2020). Modeling of heat transfer performance of carbon nanotube nanofluid in a tube with fixed wall temperature by using ANN–GA. *The European Physical Journal Plus*, *135*(2), pp.1-20.

[54] Umar, M., Raja, M. A. Z., Sabir, Z., Alwabli, A. S., & Shoaib, M. (2020). A stochastic computational intelligent solver for numerical treatment of mosquito dispersal model in a heterogeneous environment. The European Physical Journal Plus, 135(7), 1-23.

[55] Hussain, A. N., & Ismail, A. A. (2020). Operation cost reduction in unit commitment problem using improved quantum binary PSO algorithm. Int. J. Electr. Comput. Eng, 10, 1149-1155.

[56] Sibalija, T.V., (2019). Particle swarm optimisation in designing parameters of manufacturing processes: A review (2008–2018). *Applied Soft Computing*, *84*, p.105743.

[57] Özsoy, V. S., Ünsal, M. G., & Örkcü, H. H. (2020). Use of the heuristic optimization in the parameter estimation of generalized gamma distribution: comparison of GA, DE, PSO and SA methods. Computational Statistics, 35(4), 1895-1925.

[58] Yang, J., Wang, X., & Bauer, P. (2019). Extended PSO based collaborative searching for robotic swarms with practical constraints. IEEE Access, 7, 76328-76341.

[59] Mai, S., Zille, H., Steup, C., & Mostaghim, S. (2019, July). Multi-objective collective search and movement-based metrics in swarm robotics. In Proceedings of the Genetic and Evolutionary Computation Conference Companion (pp. 387-388).

[60] Qu, N., Chen, J., Zuo, J., & Liu, J. (2020). PSO–SOM neural network algorithm for series arc fault detection. Advances in Mathematical Physics, 2020.

[61] Kuntoji, G., Rao, M., & Rao, S. (2020). Prediction of wave transmission over submerged reef of tandem breakwater using PSO-SVM and PSO-ANN techniques. ISH Journal of Hydraulic Engineering, 26(3), 283-290.

[62] Mesloub, H., Benchouia, M.T., Boumaaraf, R., Goléa, A., Goléa, N. & Becherif, M., (2020). Design and implementation of DTC based on AFLC and PSO of a PMSM. Mathematics and Computers in Simulation, 167, pp.340-355.

[63] Casacio, L., Lyra, C. & Oliveira, A.R., (2019). Interior point methods for power flow optimization with security constraints. *International Transactions in Operational Research*, *26*(1), pp.364-378.

[64] Chouzenoux, E., Corbineau, M.C. & Pesquet, J.C., (2019). A proximal interior point algorithm with applications to image processing. *Journal of Mathematical Imaging and Vision*, pp.1-22.

[65] Zanelli, A., Domahidi, A., Jerez, J. & Morari, M., (2020). FORCES NLP: an efficient implementation of interior-point methods for multistage nonlinear nonconvex programs. *International Journal of Control*, *93*(1), pp.13-29.

[66] Wambacq, J., Ulloa, J., Lombaert, G., & François, S. (2021). Interior-point methods for the phase-field approach to brittle and ductile fracture. Computer Methods in Applied Mechanics and Engineering, 375, 113612.

[67] Sabir, Z., Raja, M. A. Z., Umar, M., & Shoaib, M. (2020). Design of neuro-swarming-based heuristics to solve the third-order nonlinear multi-singular Emden–Fowler equation. The European Physical Journal Plus, 135(5), 410.

[68] Sabir, Z., Umar, M., Guirao, J. L., Shoaib, M., & Raja, M. A. Z. (2021). Integrated intelligent computing paradigm for nonlinear multi-singular third-order Emden–Fowler equation. Neural Computing and Applications, 33(8), 3417-3436.

[69] Sabir, Z., Saoud, S., Raja, M. A. Z., Wahab, H. A., & Arbi, A. (2020). Heuristic computing technique for numerical solutions of nonlinear fourth order Emden–Fowler equation. Mathematics and Computers in Simulation, 178, 534-548.

[70] Sabir, Z., Umar, M., Raja, M. A. Z., Fathurrochman, I., & Hasan, H. (2022). Design of Morlet wavelet neural network to solve the non-linear influenza disease system. Applied Mathematics and Nonlinear Sciences.

[71] İlhan, E., & Kıymaz, İ. O. (2020). A generalization of truncated M-fractional derivative and applications to fractional differential equations. Applied Mathematics and Nonlinear Sciences, 5(1), 171-188.

[72] Yokuş, A., & Gülbahar, S. (2019). Numerical solutions with linearization techniques of the fractional Harry Dym equation. Applied Mathematics and Nonlinear Sciences, 4(1), 35-42.

[73] Touchent, K. A., Hammouch, Z., & Mekkaoui, T. (2020). A modified invariant subspace method for solving partial differential equations with non-singular kernel fractional derivatives. Applied Mathematics and Nonlinear Sciences, 5(2), 35-48.

[74] Sulaiman, T. A., Bulut, H., & Atas, S. S. (2019). Optical solitons to the fractional Schrdinger-Hirota equation. Applied Mathematics and Nonlinear Sciences, 4(2), 535-542.

[75] Ziane, D., Cherif, M. H., Cattani, C., & Belghaba, K. (2019). Yang-Laplace decomposition method for nonlinear system of local fractional partial differential equations. Applied Mathematics and Nonlinear Sciences, 4(2), 489-502.

[76] Yao, H., (2021). Application of artificial intelligence algorithm in mathematical modelling and solving. *Applied Mathematics and Nonlinear Sciences*.

[77] Xie, T., Liu, R. & Wei, Z., (2020). Improvement of the Fast Clustering Algorithm Improved by-Means in the Big Data. *Applied Mathematics and Nonlinear Sciences*, *5*(1), pp.1-10.

[78] Kouider, B. & Polat, A., (2020). Optimal position of piezoelectric actuators for active vibration reduction of beams. *Applied Mathematics and Nonlinear Sciences*, *5*(1), pp.385-392.

[79] Xue, Y., Sun, Q., Li, C., Dang, W. & Hao, F., (2021). Distribution network monitoring and management system based on intelligent recognition and judgement. *Applied Mathematics and Nonlinear Sciences*.